

Supporting information

Pump-Flow-Probe X-Ray Absorption Spectroscopy as a Tool for Studying Intermediate States of Photocatalytic Systems

Grigory Smolentsev, Alexander Guda, Xiaoyi Zhang, Kristoffer Haldrup, Eugen Andreiadis, Murielle Chavarot-Kerlidou, Sophie E. Canton, Maarten Nachtegaal, Vincent Artero and Villy Sundström

Time resolution

In the case of constant flow speed:

The probability density p of finding a species corresponding to the time delay t between the absorption of the optical pump and X-ray probe pulses for two beams of Gaussian shape with beam sizes described by standard deviations S_1 and S_2 is given by:

$$p(t) = \frac{v}{\sqrt{2\pi(S_1^2 + S_2^2)}} e^{-\frac{(d-vt)^2}{2(S_1^2 + S_2^2)}}, \quad (S1)$$

where d is the distance between the beams and v is the flow speed of the liquid.

Introducing unitless parameters $\gamma = \frac{t}{\tau}$ (can be interpreted as unitless time) and $\gamma_0 = \frac{d}{v\tau}$ (can be interpreted as unitless distance between beams or unitless nominal delay time), with $\tau = \frac{\sqrt{S_1^2 + S_2^2}}{v}$, the probability density, $p(\gamma)$ is a Gaussian function with standard deviation equal to $\sigma_\gamma=1$:

$$p(\gamma) = \frac{1}{\sqrt{2\pi}} e^{-\frac{(\gamma_0 - \gamma)^2}{2}}$$

The time resolution can be described by the standard deviation $\sigma = \frac{\sqrt{S_1^2 + S_2^2}}{v}$ or by the full width at half maximum (FWHM) of the distribution function,

$$\Gamma = 2.36\sigma = 2.36 \frac{\sqrt{S_1^2 + S_2^2}}{v} \quad (S2)$$

In the case of laminar flow in a cylindrical capillary:

In the case of a capillary with a non-constant flow speed, $v(r)$ as a function of the radial coordinate r , the probability density of finding a transient species corresponding to a certain delay time, $p_1(t,r)$, depend on the coordinate, r : $v(r) = v_{\max} \left(\frac{r^2}{r_0^2} - 1 \right)$, where r_0 is the radius of the capillary.

Introducing this expression into (S1) one obtains:

$$p_1(t,r) = \frac{v(r)}{\sqrt{2\pi(S_1^2 + S_2^2)}} e^{-\frac{(d-v(r)t)^2}{2(S_1^2 + S_2^2)}} \quad (\text{S3})$$

We will also take into account that more photons are absorbed by the front of the sample stream and therefore this region gives a higher contribution to the final probability distribution function $p(t)$.

If we define $W_1(r)$ ($W_2(r)$) to be the probability function describing the spatial distribution of laser (X-ray) photons absorbed at the coordinate r then we obtain,

$$p(t) = \int_r W_1(\vec{r}) W_2(\vec{r}) p_1(t,r) d\vec{r} \quad (1) \quad (\text{S4})$$

If the size of the probe beam is significantly smaller than the diameter of capillary (as in our pump-flow-probe setup) we can approximate (S4) with a one-dimensional integral:

$$p(t) = \int_{-r_0}^{r_0} A e^{-\frac{(\mu_1 + \mu_2)(r+r_0)}{2r_0}} \frac{v(r)}{\sqrt{2\pi(S_1^2 + S_2^2)}} e^{-\frac{(d-v(r)t)^2}{2(S_1^2 + S_2^2)}} dr, \quad (\text{S5})$$

where $\frac{\mu_1}{2r_0}$ ($\frac{\mu_2}{2r_0}$) is the absorption coefficient for the laser (X-ray) beam and A is a normalization constant. Introducing unitless parameters analogously to what was done for constant flow speed:

$$\gamma = \frac{t}{\tau}; \quad \gamma_0 = \frac{2d}{v_{\max}\tau}; \quad x = \frac{r}{r_0}, \quad \text{where } \tau = \frac{2\sqrt{S_1^2 + S_2^2}}{v_{\max}},$$

the probability distribution function as a function of gamma (unitless time) takes the form,

$$p(\gamma) = \frac{1}{\sqrt{2\pi}} \int_{-1}^1 \frac{(\mu_1 + \mu_2) e^{-\frac{1}{2}(\mu_1 + \mu_2)(x+1)}}{1 - e^{-(\mu_1 + \mu_2)}} (1 - x^2) e^{-\frac{1}{2}(\gamma_0 - 2(1-x^2)\gamma)^2} dx$$

The result of numerical integration of this function is shown in Fig S1

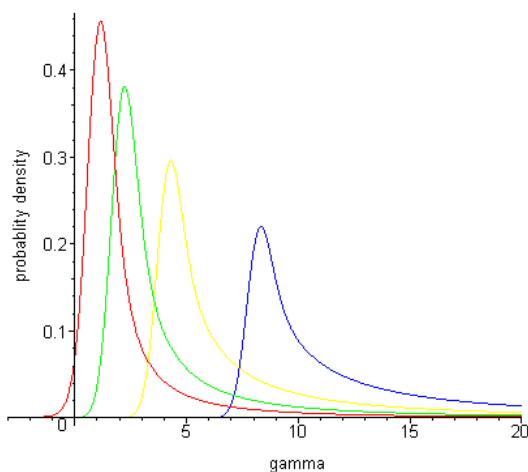


Fig. S1 Probability density for events with delay between absorption of laser and X-ray photons described by the unitless time parameter γ . The red line corresponds to the distance between laser and X-ray beams described by unitless parameter $\gamma_0=2$, the green line $\gamma_0=4$, the yellow line $\gamma_0=8$ and the blue line $\gamma_0=16$. For all the traces $\mu_1 + \mu_2 = 1.5$

Thus, as the excited sample volume moves out and away from the laser excitation region the probability distribution function $p(t)$ of excited species within a detection volume becomes increasingly skewed and accumulates more probability in a long, late time, tail (see Fig. S1). This long tail corresponds to species at a later time in the reaction cycle and leads to a mixing of “later time” species (from slowly moving sample close to the capillary walls) with “early time” species (from the center of the capillary), and therefore effectively broadens the time resolution of the experiment.

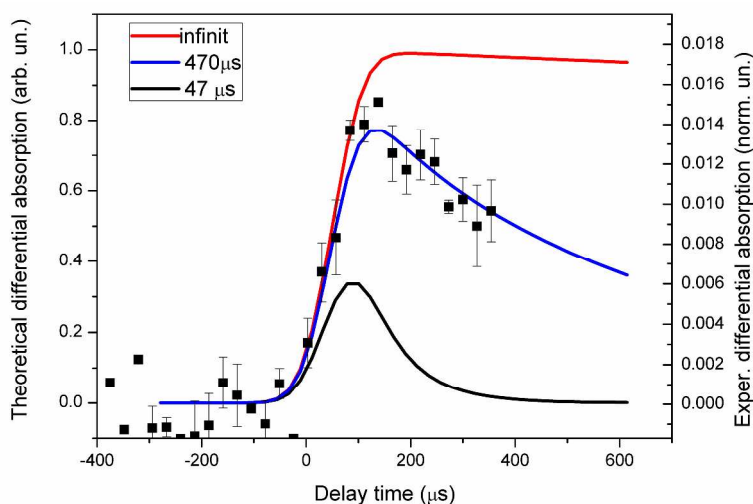


Fig. S2 Theoretical (lines) and experimental (squares) transient signals as a function of the delay time defined by the spatial separation of laser and X-ray beams. Black line corresponds to the intermediate species with the lifetime $47 \mu\text{s}$, blue line – $470 \mu\text{s}$ and red line corresponds to the limit of infinitely long lifetime.

In Fig S2 we have shown the expected transient signal as a function of the delay (analogous to those shown in Figure 4) that was simulated by convoluting the probability

distribution functions shown in Fig S1 with exponential kinetics. The signals corresponding to different lifetimes of intermediate are compared with our experimental data (the same as shown in Fig 4). In order to allow direct comparison we have shown the theoretical traces for the same parameters of the experiment (beam sizes, flow speed etc) as in Fig 4. As one can see the simulated kinetic traces depends significantly on the lifetime. Good agreement with the experiment is achieved for the model with the lifetime $\sim 470 \mu\text{s}$.

The spectrum shown in Fig. 5 in the paper was measured at a time delay corresponding to $\gamma_0 \approx 2$. From the numerical analysis of the corresponding probability density function (integration was performed up to $\gamma_{\text{max}} = 12$, which corresponds to 95% of the total probability distribution) we obtained a full width at half maximum (FWHM, Γ) of the $p(\gamma)$ distribution function of 1.6, while the standard deviation σ_γ is 2.0. The corresponding values for the time resolution for our beam sizes (FWHM of laser and X-ray beams is $100 \mu\text{m}$ and $v_{\text{max}} = 6\text{m/s}$) are $\Gamma = 32\mu\text{s}$ and $\sigma = 40 \mu\text{s}$.

Excitation conditions and time resolution - Simulations

In this section we will compare the two excitation schemes i.e. the pump-flow-probe vs. the pump-sequential probes measurement, by simulating the experiments on a multicomponent photocatalytic system consisting of $[\text{Ru}(\text{bpy})_3]^{2+}$ as the photosensitizer/chromophore, the cobaloxime $[\text{Co}^{\text{II}}(\text{dpgBF}_2)_2(\text{OH}_2)_2]$ as the final electron acceptor and MV^{2+} as an electron relay. The system does not contain any sacrificial electron donor nor proton source. The conditions were optimized to study the initial photoinduced electron transfer steps involved in the photocatalytic cycle. The concentrations are following: for the pump-flow-probe, $[\text{Ru}(\text{bpy})_3](\text{PF}_6)_2$ 0.4 mM, $\text{MV}(\text{PF}_6)_2$ 8 mM, $\text{Co}(\text{dpgBF}_2)_2(\text{OH}_2)_2$ 0.3 mM and for pump-sequential-probes, $[\text{Ru}(\text{bpy})_3](\text{PF}_6)_2$ 3 mM, $\text{MV}(\text{PF}_6)_2$ 8 mM, $\text{Co}(\text{dpgBF}_2)_2(\text{OH}_2)_2$ 1 mM. The average flow speed is 4.2 m/s. All reaction rate constants for our simulations were taken from ref. ¹¹ and they are summarized in the next section together with the rate equations.

In the pump-flow-probe experiment, the first $19 \mu\text{s}$ correspond to the photoexcitation of $[\text{Ru}(\text{bpy})_3]^{2+}$ (eq. 1) and quenching of its triplet excited state by methyl viologen (eq. 2). Therefore the concentration of $[\text{Ru}(\text{bpy})_3]^{3+}$ increases up to a saturation level of $\sim 15\%$ (see top panel of Fig. S3), that depends on the laser power. A very low level of $[\text{Ru}(\text{bpy})_3]^{2+*}$ exists during the whole time of laser illumination. The reduced viologen species, $\text{MV}^{•+}$, delivers an electron to the cobaloxime (eq. 3), producing the anionic Co(I)-complex and $[\text{Ru}(\text{bpy})_3]^{3+}$ as a net result of reactions (1)-(3). The concentration of Co(I) reaches a maximum at $65 \mu\text{s}$. In the absence of any other source of electrons, the oxidized Ru-species, $[\text{Ru}(\text{bpy})_3]^{3+}$, reacts with the Co(II)-complex (eq. 4) to form a cationic Co(III)-complex which reaches its maximum concentration at an earlier time ($30 \mu\text{s}$) than Co(I). The maximum percentage of the Co(I) and Co(III) intermediate species is 4-5.5%. Starting from $\sim 100 \mu\text{s}$ and up to 50 ms, both Co(I) and Co(III) species coexist in solution with the same concentrations and the system slowly returns to the initial state (eq 5).

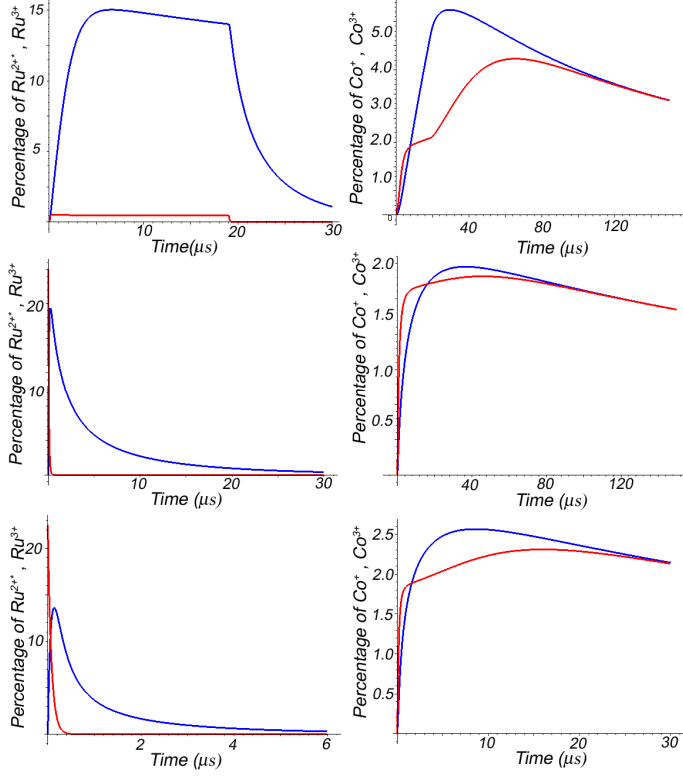
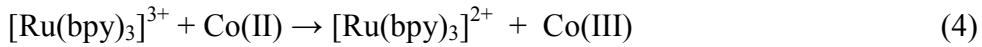
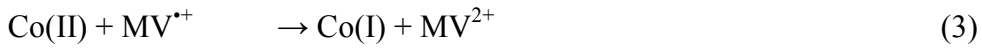
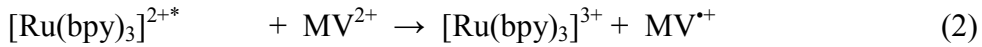


Fig.S3. Percentage of intermediate species of Ru chromophore (left) and Co species (right) as a function of time. Top panel corresponds to the concentrations optimized for the pump-flow-probe experiment, middle panel – the same concentrations but in a pump-sequential-probes scheme with pulsed excitation and bottom panel – concentrations optimized for the pump-sequential-probes experiment with pulsed excitation. Red and blue lines in the left-hand panels corresponds to $[\text{Ru}(\text{bpy})_3]^{2+*}$ and $[\text{Ru}(\text{bpy})_3]^{3+}$ respectively. In the right-hand panels red and blue lines represent Co(I) and Co(III) species respectively.



Turning next to the pump-sequential-probes experiment (middle panel of Fig. S3), the concentrations were kept unchanged compared to the pump-flow-probe experiment and only the excitation regime modified such that 30 % of the Ru-chromophores were

assumed to have been excited with a short laser pulse. In this scenario, the $[\text{Ru}(\text{bpy})_3]^{3+}$ species will be formed much earlier (and photoexcited $[\text{Ru}(\text{bpy})_3]^{2+*}$ will decay almost instantaneously on the time scale used in Fig. S3). The concentrations of the Co(I) and Co(III) species will reach a maximum of almost 2 %. By comparing the upper and middle right-hand panels of Fig. S3 we conclude that the CW excitation scheme should give a higher percentage of Co(I) and Co(III) intermediates at these particular excitation conditions.

The available excitation wavelength of the pulsed laser is 527 nm (in contrast to 447 nm for the CW laser) and the optical density for $[\text{Ru}(\text{bpy})_3]^{2+}$ (with a realistically achievable jet diameter of ~ 1 mm) is low (~ 0.05) and 90 % of the laser photons are not absorbed in the sample. With the conditions optimized for the pump-sequential-probes experiment (3 mM of $[\text{Ru}(\text{bpy})_3]^{2+}$ and 1 mM of cobaloxime), a somewhat higher concentration of intermediate Co species (2-2.5 %) is obtained and the charge transfer to the Co species will be much faster (see lower panels of Fig. S3 and note that the time scale is different). Therefore, in order to investigate the same states using the pump-sequential-probes setup a much higher time resolution is required (in comparison to the pump-flow-probe experiment). In the pump-flow-probe experiment the flow speed and the laser spot size define not only the time resolution but also the number of absorbed photons, and therefore the fraction of excited chromophores. For example, increase of the flow speed up to 8.4 m/s will decrease the maximal percentage of the Co(III) intermediate to 3.5%

Reaction rate constants and differential equations describing reaction kinetics

$$\frac{d\text{Ru}^{2+*}}{dt} = f(t)(1 - 10^{-\varepsilon d([\text{Ru}^{2+}] - [\text{Ru}^{2+*}] - [\text{Ru}^{3+}])}) - k_1[\text{Ru}^{2+*}] - k_2[\text{Ru}^{2+*}][\text{MV}^{2+}]$$

$$\frac{d\text{MV}^{2+}}{dt} = -k_2[\text{Ru}^{2+*}][\text{MV}^{2+}] + k_3[\text{Ru}^{3+}][\text{MV}^{+}] + k_4[\text{Co}^{2+}][\text{MV}^{+}] + k_7[\text{Co}^{3+}][\text{MV}^{+}]$$

$$\frac{d\text{Ru}^{3+}}{dt} = k_2[\text{Ru}^{2+*}][\text{MV}^{2+}] - k_3[\text{Ru}^{3+}][\text{MV}^{+}] - k_5[\text{Co}^{+}][\text{Ru}^{3+}] - k_6[\text{Ru}^{3+}][\text{Co}^{2+}]$$

$$\frac{d\text{MV}^{+}}{dt} = k_2[\text{Ru}^{2+*}][\text{MV}^{2+}] - k_3[\text{Ru}^{3+}][\text{MV}^{+}] - k_4[\text{Co}^{2+}][\text{MV}^{+}] - k_7[\text{Co}^{3+}][\text{MV}^{+}]$$

$$\frac{d\text{Co}^{2+}}{dt} = -k_4[\text{Co}^{2+}][\text{MV}^{+}] + k_5[\text{Co}^{+}][\text{Ru}^{3+}] - k_6[\text{Ru}^{3+}][\text{Co}^{2+}] + k_7[\text{Co}^{3+}][\text{MV}^{+}] + 2k_8[\text{Co}^{3+}][\text{Co}^{+}]$$

$$\frac{d\text{Co}^{+}}{dt} = k_4[\text{Co}^{2+}][\text{MV}^{+}] - k_5[\text{Co}^{+}][\text{Ru}^{3+}] - k_8[\text{Co}^{3+}][\text{Co}^{+}]$$

$$\frac{d\text{Co}^{3+}}{dt} = k_6[\text{Ru}^{3+}][\text{Co}^{2+}] - k_7[\text{Co}^{3+}][\text{MV}^{+}] - k_8[\text{Co}^{3+}][\text{Co}^{+}]$$

$$f(t) = \begin{cases} \frac{N}{V N_A} & 0 < t < \tau \\ 0 & \text{if } t < 0, t > \tau \end{cases}$$

$f(t)$ - describes photoexcitation by the laser: N – number of laser photons at the sample position per unit of time, V – irradiated volume, N_A – Avogadro constant, τ – time of laser irradiation of each elementary volume of sample, ε – extinction coefficient of the sample, d – thickness of the sample

Table S1: Reaction rate constants:

| | |
|----------------|--|
| k ₁ | 1.04*10 ⁶ s ⁻¹ |
| k ₂ | 1.58*10 ⁹ M ⁻¹ s ⁻¹ |
| k ₃ | 5.7*10 ⁹ M ⁻¹ s ⁻¹ |
| k ₄ | 2*10 ⁸ M ⁻¹ s ⁻¹ |
| k ₅ | 9.8*10 ⁹ M ⁻¹ s ⁻¹ |
| k ₆ | 5.2*10 ⁷ M ⁻¹ s ⁻¹ |
| k ₇ | 6*10 ⁶ M ⁻¹ s ⁻¹ |
| k ₈ | 4.4*10 ⁸ M ⁻¹ s ⁻¹ |

Summary of experimental conditions and details of calculations relevant for the estimation of the statistics of photons presented in Table 1

- Total number of fluorescent photons/s, N, was estimated using the following formula:

$$N = \frac{N_0 \mu_A(E)}{\mu_T + \mu_F} \left[1 - e^{-(\mu_T + \mu_F)D} \right]$$

where N₀ – number of incident photons on the sample; $\mu_A(E)$ – absorption coefficient for the edge of interest; μ_T – absorption coefficient by all atoms of the sample (including solvent) for the energy of incident beam; μ_F – absorption coefficient by all atoms of the sample (including solvent) for the energy of fluorescence; D – diameter of the jet. Absorption coefficients were calculated taking into account that the pump-sequential-probes spectra shown in Figs. 3 and 5 in the paper correspond to a Co-concentration of 1 mM, whereas for the pump-flow-probe experiment the Co concentration is 0.7 mM.

- The total count rate of the detector in the pump-flow-probe experiment is limited by the detector saturation level. The Ge detector with 12-13 channels allows detection of a maximum of 5*10⁴ photons/(channel*s). The total count rate in the case of the pump-sequential-probes experiment is defined by the area of the APD detector and the reduction of the radiation by the Z-1 filters and Soller slits.
- The total counts/s of the detector for each time point for the pump-sequential probes experiments was calculated taking into account that the time between X-ray pulses in the 24 bunch mode at APS is 153 ns, while the time between laser pulses is 1 ms.
- The pump-flow-probe method measures only one time point using the full flux. The region of interest for the detector was selected around the Co K-alpha line. For a concentration of 0.3 mM the count rate is 7.8*10⁴ counts/s.

- For both experiments the counts of the detector consist of the background counts N_b , that are observed also for an incident x-ray energy below the absorption edge, and fluorescent counts N_f . The number of detected fluorescent counts for a 0.3 mM concentration is $1.8 \cdot 10^4$.

- The effective number of counts, $N_{eff} = \frac{N_f^2}{N_f + N_b}$, corresponds to the number of

counts that gives the same signal/noise ratio (S/N) with the signal without any background. The formula follows from the estimation of signal-to-noise ratio for our spectrum. Shot noise after the absorption edge is the square root of the total counts that we observe: $Noise = \sqrt{N_b + N_f}$. The useful signal is N_f . Therefore, the signal-to-

noise ratio for the fluorescence spectrum is $Signal / Noise = \frac{N_f}{\sqrt{N_b + N_f}}$. By definition,

N_{eff} is the number of photons that has to be registered in order to achieve the same signal-to-noise ratio with an ideal detector that does not register any background. In

other words, for the ideal detector, $Signal / Noise = \frac{N_{eff}}{\sqrt{N_{eff}}} = \sqrt{N_{eff}}$, from which the

formula introduced above follows.

- For the pump-flow-probe experiment the “laser on” signal was measured for 30 s and then the “laser off” signal was measured for the same time.
- For the pump-sequential-probes experiment the S/N of the detector measuring the sample signal (I) was $2.1 \cdot 10^{-3}$ and the S/N of the incoming intensity detector (I_0) was $6 \cdot 10^{-4}$. Laser off spectra were measured by averaging 20 spectra that precede the laser pulse.
- For the pump-flow-probe experiment, laser off and laser on spectra have the same noise, $2.9 \cdot 10^{-4}$, and equally contribute to the noise of the difference spectrum. Contribution of the noise of the I_0 detector to the noise of the difference spectrum is negligible.
- For calculation of the laser dose we have taken into account that for the pump-flow-probe experiment the laser is off half of the time, while it is always on for pump-sequential-probes experiment.

Spectra of reference compounds:

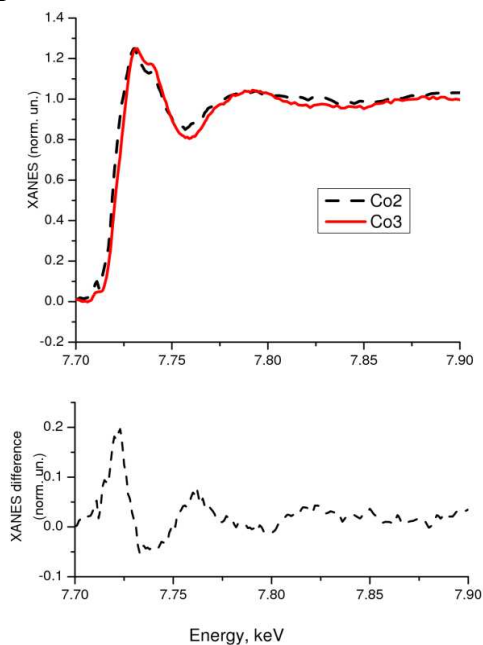


Fig. S4. Top panel: ground state XAS spectra of the Ru/MV/Co sample (black dashed line) and chloro(pyridine)bis(dimethylglyoximato)Cobalt(III) (Co(III), red solid line) Bottom panel : difference between spectra of Ru/MV/Co and Co(III)

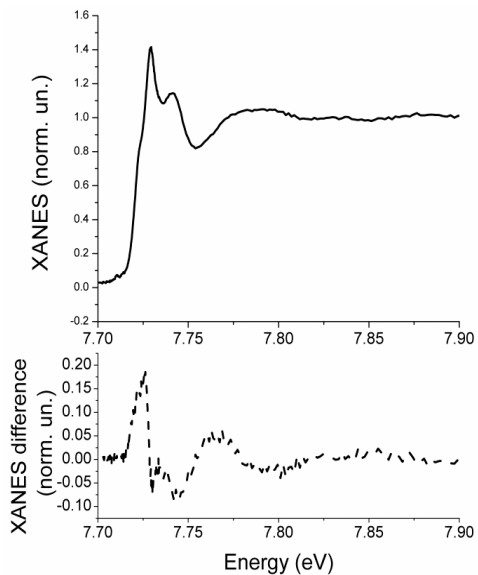


Fig S5 Reference spectrum for Co(III) reduction obtained from measurements on a supramolecular RuCo complex (for details see ref 17) with Co(bpy)₃ type of Co environment. Upper panel: ground state spectrum with Co(III) in the ground state. Lower panel: transient spectrum corresponding to Co(III) to Co(II) reduction

Reference compounds with Co(I) and a similar ligand system are very unstable and therefore it is extremely difficult to obtain such a reference spectrum.

Radiation damage

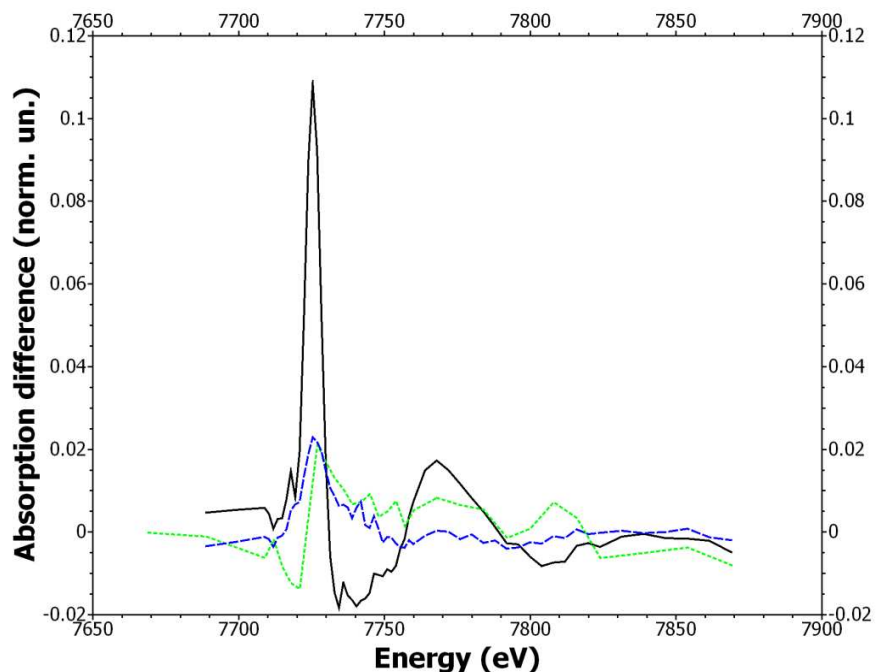


Fig S6 Damage-related spectra for three different exposure regimes. Difference between Co K-edge XANES of partially damaged and the initial Ru/MV/Co sample is shown. Green (short dash line): the spectrum was measured using the pump-flow-probe method and corresponds to a dose of $3.2 \cdot 10^{22}$ laser photons and $1.1 \cdot 10^{16}$ X-ray photons; the volume of the sample is 90 ml. Black (solid line): the spectrum was measured using the pump-sequential-probes method and corresponds to a dose of $1.6 \cdot 10^{22}$ laser photons and $7.6 \cdot 10^{16}$ X-ray photons; the volume of the sample is 45 ml. Blue (dashed line): the spectrum was measured using the pump-sequential-probes method and corresponds to a dose of $1.2 \cdot 10^{21}$ laser photons and $5.5 \cdot 10^{15}$ X-ray photons; the volume of the sample is 45 ml.

The green and black spectra have the same dose of laser radiation per ml of sample, but the dose of X-ray radiation for the black spectrum is ~ 13 times higher. Blue and green spectra have the same X-ray dose, but the dose of laser radiation for the green sample is ~ 13 times higher. From this we conclude that the x-ray radiation is the main source of sample degradation.

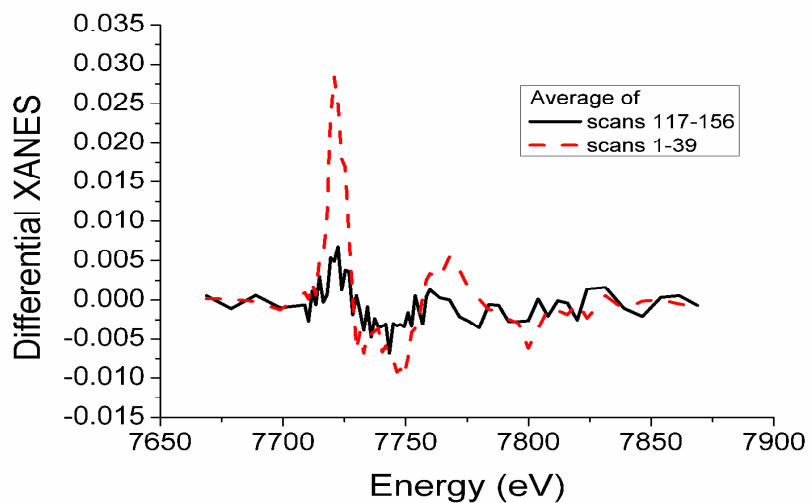


Fig S7. Influence of the radiation damage on the transient XAS spectrum measured using the pump-sequential-probes method. Scans 1-39 correspond to a relatively fresh sample, while scans 117-156 correspond to the significantly damaged sample. Each scan corresponds to 60 points with 4 s of accumulation per point. These results show that the main effect of sample degradation is a decrease of signal amplitude.